Self-Organized Molecular Films with Long-Range Quasiperiodic Order

Vincent Fournée,[†,*] Émilie Gaudry,[†] Julian Ledieu,[†] Marie-Cécile de Weerd,[†] Dongmei Wu,[‡] and Thomas Lograsso[‡]

[†]Institut Jean Lamour, UMR 7198 CNRS-Université de Lorraine, Parc de Saurupt, 54042 Nancy Cedex, France and [‡]The Ames Laboratory, Iowa State University, Ames, Iowa 50011, United States

ABSTRACT Self-organized molecular films with long-range quasiperiodic order have been grown by using the complex potential energy landscape of quasicrystalline surfaces as templates. The long-range order arises from a specific subset of quasilattice sites acting as preferred adsorption sites for the molecules, thus enforcing a quasiperiodic structure in the film. These adsorption sites exhibit a local 5-fold symmetry resulting from the cut by the surface plane through the cluster units identified in the bulk solid. Symmetry matching between the C_{60} fullerene and the substrate leads to a preferred adsorption configuration of the molecules with a pentagonal face down, a feature unique to quasicrystalline surfaces, enabling efficient chemical bonding at the molecule–substrate interface. This finding offers opportunities to investigate the physical properties of model 2D quasiperiodic systems, as the molecules can be functionalized to yield architectures with tailor-made properties.

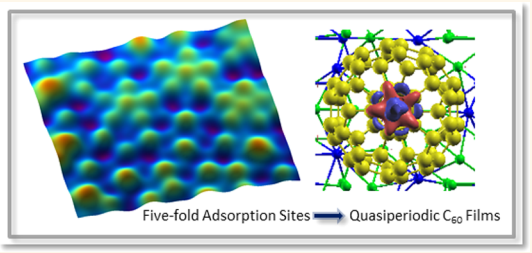

KEYWORDS: C_{60} · self-assembly · quasiperiodic order · scanning tunneling microscopy · density functional theory · 5-fold symmetry

Quasicrystals (QCs) were discovered in intermetallic compounds by D. Shechtman, Nobel Prize in Chemistry 2011.[1] They possess long-range order but no translational invariance. They are a special class of complex intermetallics, in the sense that their unit cell is of infinite dimension. QCs have a fascinating beauty associated with forbidden symmetries, like five-, 10-, or 12-fold rotational symmetries not found in periodic systems. Today, the field is very active, and QCs are being discovered in a broad range of systems. Hundreds of intermetallic compounds with quasiperiodic structures have been identified in phase diagrams.[2] But QCs are no longer restricted to intermetallics. Soft QCs are an emerging field in colloidal and supramolecular chemistry.[3,4] Perovskite oxide thin films with quasiperiodic structures have recently been identified,[5] and even water thin films have been predicted to adopt quasiperiodic structures under specific conditions.[6] In this article, we show that molecular films with long-range quasiperiodic order can also be grown by using clean QC surfaces as templates, thus extending the concept of QCs to an even wider materials field.

Thorough investigations of QC surfaces in an ultra-high-vacuum environment have led to the conclusion that they are bulk terminated at specific planes.[7,8] For Al-based QCs, the selected terminations are dense Al-rich planes of the bulk structure separated by the largest interplanar distances corresponding to the lowest surface energy terminations. Low-energy electron diffraction (LEED) and scanning tunneling microscopy (STM) images reveal both the long-range quasiperiodic order and local atomic configurations corresponding to cluster building blocks used to described the bulk structure that are truncated by the surface plane.[9−12] Such terminations represent a complex potential energy landscape for any adsorbate landing on the surface. Nucleation and growth experiments of metal thin films indicated a heterogeneous nucleation mechanism at specific quasilattice sites acting as "trap" sites for the adatoms.[13] These trap sites may depend on the adsorbate, but, in most cases, they have been identified as local configurations resulting from bulk clusters intersected by the surface plane, either Bergman or Mackay clusters in the case of icosahedral (*i*)−Al−Pd−Mn or

* Address correspondence to vincent.fournee@univ-lorraine.fr.

Received for review January 14, 2014 and accepted March 20, 2014.

Published online March 20, 2014
10.1021/nn500234j

i–Al–Cu–Fe phases.[13–15] In specific cases, the mechanism of preferential adsorption at trap sites leads to a pseudomorphic growth of the metal thin film, which is limited to the first layer(s). This has been observed for a few low-melting-point elements such as Pb and studied both experimentally and using simulations based on density functional theory (DFT) calculations.[16–18]

A quasiperiodic molecular overlayer would be even more interesting, as the molecules can be functionalized to yield model 2D systems with specific properties. However earlier attempts to produce such films failed due to the fact that the molecules strongly bond at the surface, leading to disordered structures, although some indications of preferred adsorption sites were reported at very low coverages.[19,20]

In this article, we report the successful growth of well-ordered self-organized molecular films on different QC substrates, achieved by high-temperature deposition. There is a delicate balance to fulfill because the deposition temperature should be high enough to induce sufficient diffusion of the molecules on the substrate while still being low enough to avoid polymerization or any other molecular transformations. We first describe the structure of the molecular films formed on different QC substrates as observed by LEED and STM. A detailed analysis of the pattern formed by the molecules indicates that they preferentially adsorb at 5-fold symmetric sites on the different substrates, thus defining an ordered inflated quasilattice with some disorder intrinsic to quasiperiodic structures. Then we describe the adsorption geometry of the molecules on the QC substrates based on DFT calculations. The bonding charge density at the molecule/substrate interface indicates covalent-like interaction, and the lowest adsorption configurations are achieved for C_{60} molecules contacting the surface with a pentagonal face to match the surface symmetry, a feature unique to QC surfaces.

RESULTS AND DISCUSSION

Molecular films were grown by exposing the surface of Al-based QCs to a multilayer of C_{60}, while maintaining the substrate temperature within a temperature window ranging from 623 to 673 K. This temperature range is above the multilayer desorption temperature; therefore only the first layer remains on the surface. We also checked that no change in the C 1s core level line shape was observed by photoemission spectroscopy upon annealing a single layer of C_{60} up to 700 K, indicating that no polymerization or fragmentation of the molecules takes place in this temperature range. Figure 1a shows a LEED pattern of the 10-fold surface of the decagonal (*d*)–Al–Ni–Co QC before deposition. It is characterized by rings of 10 diffraction spots of equal intensity having radius scaling as a power of the golden mean τ. The LEED pattern of the molecular film (Figure 1b) shows similar characteristics, but the number of intense diffraction rods intercepted by the Ewald sphere is larger. It indicates that the C_{60} monolayer has self-organized into a 10-fold symmetric pattern. A similar diffraction pattern was observed for C_{60} films grown on the 10-fold surface of the *d*–Al–Cu–Co phase. The real space structure of the film is shown in Figure 1c, where each molecule appears as a bright dot in the STM image. The small contrast variations correspond to a height difference ranging from 0.1 to 0.2 nm. Roughness analysis of STM images recorded at

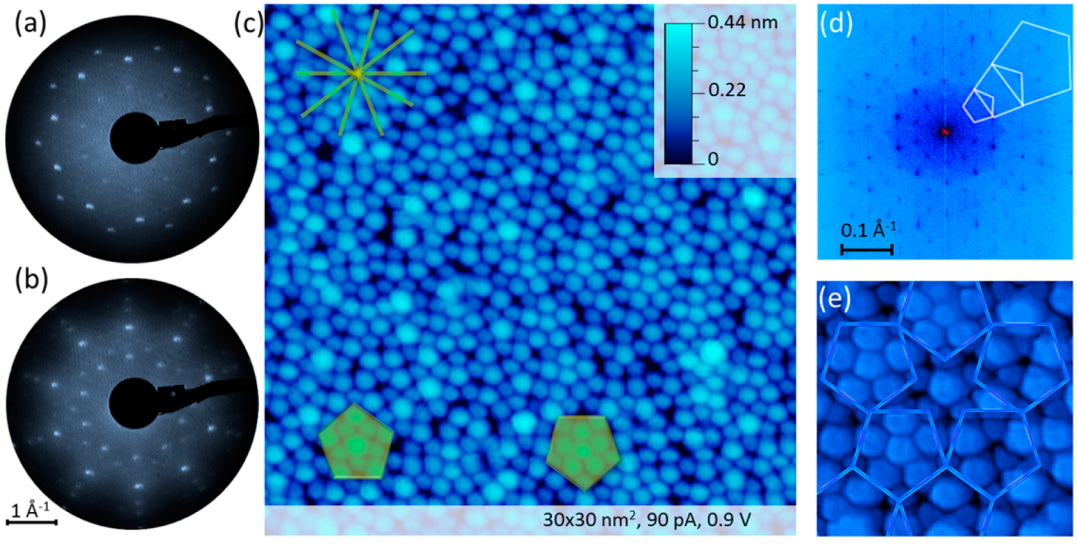

Figure 1. (a) LEED patterns of the clean 10-fold surface of the Al–Ni–Co decagonal phase and (c) of the C_{60} film formed on that surface. Both patterns were recorded at an incident beam energy of 48 eV. (c) STM image of the C_{60} monolayer formed on the 10-fold surface of the Al–Cu–Co decagonal phase. The preferred alignment directions as well as the most frequent local configurations are highlighted in yellow. (d) FFT of the STM image showing several rings of 10 spots and τ-scaling relationships. (e) Portion of the P1 tiling with 2 nm edge length superimposed on an STM image.

different voltages provides evidence for a bias dependence of the STM contrast (from −2 V to +2 V). The film is compact, except for a few vacancies. The average surface area per molecule is estimated at 1.0 ± 0.05 nm^2, corresponding to a slightly lower density than that of a perfectly ordered hexagonal close-packed layer adopting a C_{60} bulk nearest-neighbor distance of 1.004 nm (surface area per molecule: 0.873 nm^2). The fast-Fourier transform (FFT) of the image shows several rings of 10 spots, consistent with the LEED pattern and confirming the long-range quasiperiodic order of the film (Figure 1d). The autocorrelation of the STM image also attests to the structural quality of the film. The nearest-neighbor (NN) distance is 1.01 ± 0.01 nm, similar to NN distances typically observed in hexagonal close-packed C_{60} monolayers on metal surfaces. The molecules appear to be aligned preferentially along lines that are rotated by 36° from each other in accordance with the 10-fold rotational symmetry of the film (Figure 1c). For a specific direction, parallel lines are separated by different distances having a τ-scaling relationship. The most frequent local configurations are highlighted in Figure 1c. They are pentagonal tiles with an edge length of 2.0 ± 0.1 nm. The tiles are usually decorated by a smaller pentagon rotated by $2\pi/5$ with an edge length of 1.2 ± 0.1 nm plus a central molecule. The pentagonal tiles can have two orientations on the same terrace, pointing either up or down.

The pattern formed by the molecules can be understood in light of the surface model of the *d*−Al−Cu−Co phase. The crystallographic structure of this phase has been investigated by high-resolution transmission electron microscopy (TEM) and X-ray diffraction.[21] Several variants of the bulk structure model have been proposed, because different phases exist for different chemical compositions and in view of the difficulty in distinguishing Cu and Co atoms by X-ray diffraction or TEM. However, a robust feature common to all Al-based decagonal QCs is their description as 2D dense packing of partially overlapping columnar clusters. The clusters are 2 nm in diameter and extend along the 10-fold rotational axis (*i.e.*, perpendicular to the surface plane). The atomic arrangement within the 2 nm clusters has 5-fold symmetry rather than 10-fold.[21] In particular, pentagonal atomic arrangements distributed at the node of a pentagon with edge length equal to 1.2 nm decorate their interior. Within the 10-fold planes, the cluster centers form the vertices of a 2D quasiperiodic tiling with decagonal symmetry used to describe the structure. A first report on the structure of the 10-fold Al−Cu−Co surface concluded that it is bulk terminated.[22] The same surface has been reinvestigated recently using different techniques, and it was concluded that the top surface layer is Al enriched compared to the bulk composition.[23] Nevertheless, STM images show geometrical features consistent with a truncated bulk structure, with 2 nm clusters decorating the nodes of a decagonal tiling.

It is striking to note that the dimensions of the pentagonal tiles formed by the molecular film exactly match the dimensions of the underlying quasiperiodic tiling. This suggests that the C_{60} molecules preferentially adsorb at 5-fold symmetric sites, as shown in the model proposed in Figure 2. The atomic structure of the *d*−Al−Cu−Co QC in the 10-fold plane is shown. One basic cluster unit is outlined, together with the 2 nm edge length quasiperiodic tiling connecting the cluster centers. The tiling consists of pentagon, boat, and star units (so-called P1 tiling). The observed molecular pattern can be reproduced by placing C_{60} molecules at each cluster center on this model. Inside a pentagonal tile with an edge length of 2 nm, five additional molecules can be located on top of locally 5-fold symmetric sites, defining a smaller pentagon with an edge length of 1.2 nm, plus an additional one at the center. This reproduces exactly the most frequent motifs observed in STM images, *i.e.*, a 2 nm edge length pentagonal tile decorated with a smaller centered pentagonal motif having a 1.2 nm edge length and pointing in the opposite direction. A fraction of the P1 tiling has been overlapped on the experimental image of the molecular film in Figure 1e. An excellent agreement is found with the proposed model—even the star-shaped tile is reproduced in detail—although there is some disorder in the experimental system (*e.g.*, decoration of the pentagonal tile not completely

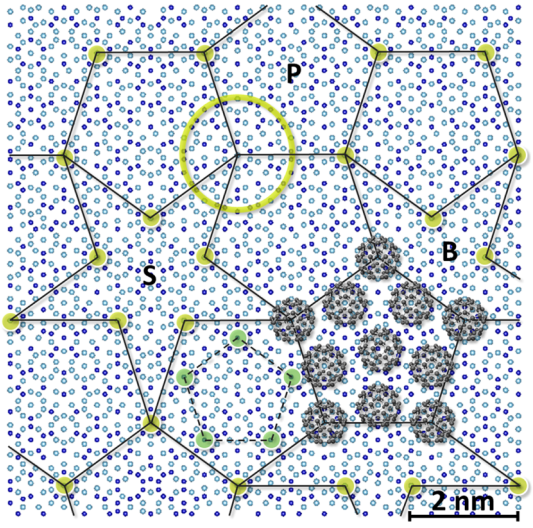

Figure 2. Model of the *d*−Al−Cu−Co phase perpendicular to the 10-fold axis. Al atoms appear as light blue circles and transition metal atoms (Cu/Co) as dark blue circles. The cluster centers are highlighted as yellow circles. The yellow ring delimits the 2 nm wide cluster units. The tiling connecting the cluster centers appears as dark lines. It consists of pentagonal (P), star (S), and boat (B) tiles with 2 nm edge lengths. The green circles inside the P tile at the bottom of the figure indicate additional 5-fold symmetric sites. They define a smaller pentagon with an edge length of 1.2 nm (dotted dark line). The decoration of the P tile by C_{60} molecules (in gray) is illustrated.

achieved in some cases). We also note that the C_{60} molecules adsorbed on top of cluster centers (*i.e.*, at the nodes of the P1 tiling) have a darker contrast compared to C_{60} adsorbed at other sites, indicating a different adsorption configuration. This may be due to differences in the configuration of the adsorption sites and/or to different orientations of the molecules with respect to the surface and/or to a different bonding with the substrate.

Molecular films with long-range quasiperiodic order can also be formed on 5-fold surfaces of *i*−Al−Cu−Fe and *i*−Al−Pd−Mn QCs. These two phases are described by the same structural model, although the chemical decoration is different.[24] If sufficient thermal energy is provided during the growth, the molecules can diffuse at the surface before being trapped by some preferred adsorption sites, and a well-ordered layer of C_{60} molecules is obtained. This is demonstrated by STM images and LEED patterns in Figure 3. Like for the clean surface, the diffraction pattern of the molecular film has 5-fold symmetry and is aperiodic, with diffraction spot positions presenting τ-scaling relationships. The number of intense diffraction spots for a given beam energy is larger compared to the clean surface. The local atomic structure of the film is revealed by STM images (Figure 3a). Bias dependence of the STM contrast shows that there are (at least) two types of adsorption configurations. At positive bias, all molecules appear to have the same height, while at negative bias bright and dim molecules can be clearly distinguished, with a height difference equal to 0.1 nm. The FFT and autocorrelation of STM images demonstrate the structural quality of the film (not shown). The shortest intermolecular distance is again 1 nm. The most frequent local configurations are highlighted in Figure 3c. They are pentagonal motifs having 1.2 nm edge lengths centered by either a bright (b) or a dim (d) C_{60}. We call these pentagonal motifs B and D (see Figure 3c). The B and D motifs are pointing in opposite directions on a same terrace, and they keep the same orientation across different terraces. Similar observations were made for C_{60} films on the *i*-Al−Pd−Mn substrate.

Here again, the pattern formed by the molecules can be understood in light of the structure model of the 5-fold surface (Figure 4a).[25] The most frequent local atomic configurations recognized in STM images of the clean surface are outlined. They are the white flower (WF) and the dark star (DS) motifs. The WF motifs correspond to Mackay clusters truncated in their equatorial plane or hanging down from the surface plane.[9,10] The DS motifs correspond to truncated Bergman clusters or truncated Mackay clusters with a central vacancy.[9,10] The tiling connecting the WF centers is called the τP1 tiling.[17] It has an edge length of 1.26 nm and consists of pentagons (P), stars (S), and rhombi (R) tiles. The P tiles point in either the upward or downward direction. The P tiles having a DS motif in their center are all pointing in the upward direction in the model (Figure 4a). Other P tiles contain more Al atoms in their interior. The dimensions of the P tiles are similar to the dimensions of the B and D motifs realized by the C_{60} molecules. This indicates that the 5-fold symmetric sites at WF motifs act as trap sites for the C_{60} molecules, enforcing the formation of the pentagonal B and D molecular features. The DS motifs are additional potential adsorption sites with local 5-fold symmetry. Because they correspond to a vacancy site, it is reasonable to assume that C_{60} adsorbed on a DS motif will appear with a darker contrast, potentially explaining the pentagonal motifs of type D. In addition, the D motifs always

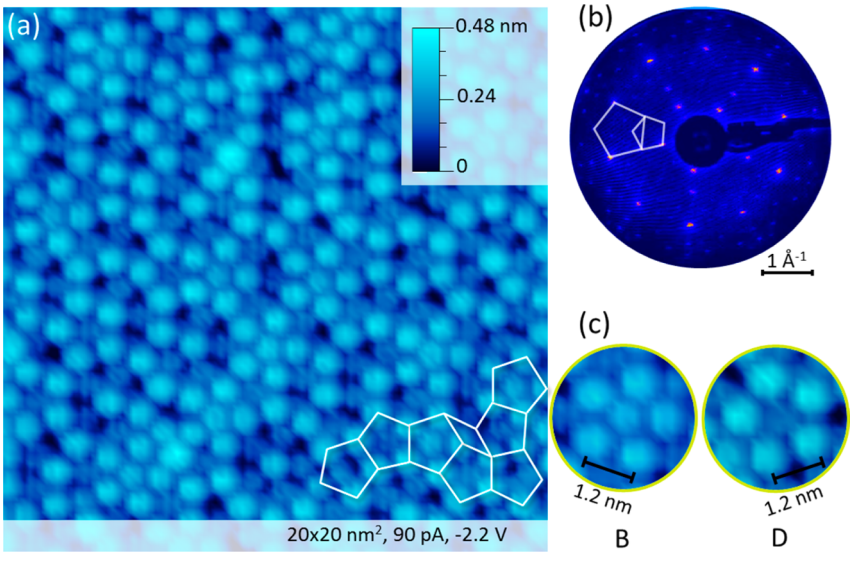

Figure 3. (a) STM image of the C_{60} monolayer formed on the 5-fold surface of the Al−Cu−Fe icosahedral QC and (b) the corresponding LEED pattern recorded at an incident beam energy of 43 eV demonstrating the 5-fold symmetry of the film. The most frequent local configurations are shown in (c). A portion of the quasiperiodic tiling is overlapping the STM image in (a).

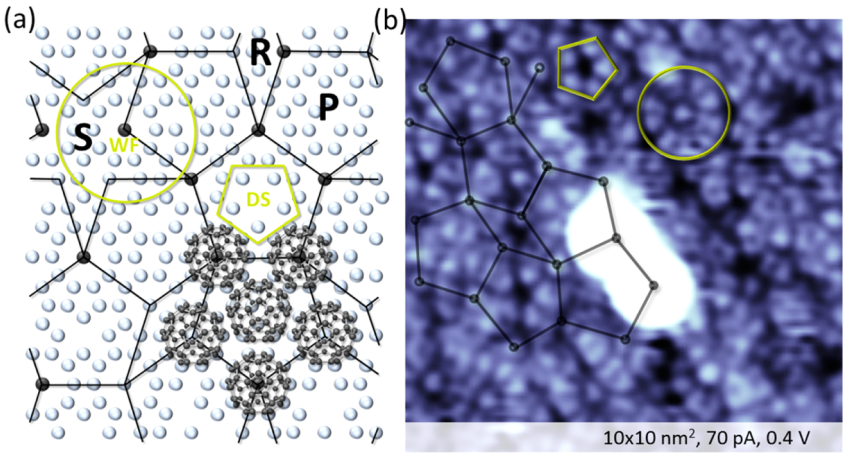

Figure 4. (a) Model of the 5-fold surface of the Al−Pd−Mn QC. Only the atoms of the top plane are shown. Al atoms appear as light gray circles and Mn atoms as dark gray circles. The WF and DS motifs are highlighted in yellow. The tiling connecting the WF centers has an edge length of 1.26 nm and is shown as dark lines. It consists of pentagons (P), stars (S), and rhombi (R) tiles. A decoration of the P tiles by C_{60} molecules (small gray circles) is shown. (b) STM image of the 5-fold surface of the Al−Pd−Mn icosahedral QC. The WF (circle) and DS (pentagon) motifs can be easily recognized, allowing the construction of the quasiperiodic tiling. The two adjacent bright dots are individual C_{60} molecules, occupying the node of a P tile.

appear with the same orientation, a characteristic that is shared with DS motifs. Other P tiles with no vacancy site in their center should thus correspond to B motifs. The density of dim C_{60} has been estimated from STM images and is about 0.25 to 0.3 per nm^2. These numbers are similar to the average density of DS sites estimated from bulk structure models of the *i*−Al−Pd−Mn QC, giving further support to our interpretation.[10] In addition, the shortest distance between two dim molecules is about 1.2 nm, corresponding to the frequent distance between two DS sites.

All these experimental observations converge toward the interpretation that dim molecules are C_{60} adsorbed at DS sites, while bright molecules are adsorbed at WF sites, defining the nodes of the inflated τP1 tiling. The decoration of the tiling by C_{60} according to this model reproduces the basic ingredients of the molecular film structure. However, it generates unrealistically short intermolecular distances. For example, the two sites connected by the short diagonal of the R tile (Figure 4a) cannot be occupied simultaneously, as it would generate an NN distance of 0.78 nm between two C_{60}, which is too short. This introduces some disorder in the decoration of the inflated quasilattice. This disorder is not of positional type but is due to the fractional occupancy of some of the trap sites of the quasilattice, because of a closeness condition between two adjacent molecules (*i.e.*, the distance between two C_{60} should not be smaller than about 0.9 nm due to repulsive van der Waals interactions). Note also that the molecular film results in the decoration of a unique quasilattice; therefore there are no boundaries resulting from the coalescence of overlayer domains or islands.

STM images of the substrate at submonolayer coverage provide additional support to the structure model (Figure 4b). The structure of the QC surface can clearly be resolved, and one can connect the WF centers to build part of the τP1 tiling with a 1.26 nm edge length. Individual C_{60} molecules appear as bright spots located most frequently at the node of this tiling or at the center of the P tiles, thus confirming the determination of the preferred adsorption sites as WF and DS motifs.

To get further insight into the adsorption mechanism, structural, energetics, and electronic structure calculations have been performed within the DFT framework using dispersion-corrected functionals.[26,27] The surface model is constructed from a cut through a bulk structure model of a 2/1 rational approximant to the Al−Pd−Mn icosahedral QC as explained by Krajčí *et al.*[25] The 2/1 approximant is obtained by the cut-and-projection technique using the Katz−Gratias−Boudard model of the bulk QC phase.[24] The slab model of the surface contains 205 atoms per cell, and the surface cell contains both WF and DS motifs. The adsorption energies of a C_{60} molecule on these two sites have been calculated for several likely adsorption geometries. Among the configurations considered, the two most stable ones correspond to a C_{60} adsorbed with a pentagonal face on top of either a WF or a DS motif. In the case of the DS site, the lowest adsorption energy ($E_{ad} = -3.20$ eV) is found when the pentagonal face of the C_{60} is aligned with the pentagon formed by the five Al atoms of the DS. A rotation of the molecule by 36° around the surface normal (C and Al pentagons pointing in opposite directions) leads to a far less stable configuration ($E_{ad} = -1.57$ eV). The adsorption energy on the WF sites is slightly higher than on DS sites ($E_{ad} = -2.90$ eV) and is much less sensitive to the relative orientation (either aligned or in head to tail configuration) of the C pentagonal face with respect to the Al pentagonal motif lying slightly below the central Mn atom. On both sites, adsorption configurations of the

C_{60} with a hexagonal face down or on a C−C bond are much less stable (E_{ad} ranging from −2.29 to −1.61 eV). The calculated distance between the centroid of the C pentagonal face and the Mn central atom of the WF is 0.173 to 0.177 nm depending on the azimuthal angle. When adsorbed at the DS site, the C_{60} molecule lies closer to the surface (distance between the centroids of the surface Al pentagon and the C pentagonal face = 0.109 nm). This supports our interpretation that the dim molecules are C_{60} adsorbed at DS sites, while C_{60} adsorbed at WF sites would appear brighter in STM images.

To get insight into the bonding mechanism, the charge density differences have been calculated to show how the charges are redistributed upon C_{60} adsorption. The charge density difference is obtained by subtracting the densities of the bare surface and the isolated C_{60} monolayer from the density of the adsorbate−substrate system. The results are shown in Figure 5 for the two most stable configurations and for a meaningful value of the charge density isosurface. When a C_{60} is adsorbed on a DS site (Figure 5a), the bonding charge density is mainly localized between five C atoms and the five Al atoms of the DS as well as in the region directly underneath the C_{60}. The charge accumulation is rather directional along the C−Al bonds. Note that the C atoms involved are not those forming the pentagonal face but lateral C atoms involved in adjacent 6:6 bonds connecting the surrounding five hexagonal facets. When adsorbed on a WF site, the bonding charge is mainly localized in the interface region between the C pentagonal face and the Mn atom located at the center of the WF motif (Figure 5b). The largest electron accumulation zone lies below the C pentagonal face in the interfacial plane and is bracketed by electron depletion zones above and below. The 5-fold symmetry of the electron density redistribution is obvious for both adsorption sites. The change in the electron density is mostly confined to the top surface layer, the bottom part of the C_{60}, and the interface region. These charge density differences suggest a covalent or iono-covalent character of the bond between the molecule and the substrate.

The calculated projected densities of states (PDOS) on C_{60} before and after adsorption are shown in Figure 5c and d. At DS sites, the shape and/or positions of the highest occupied and lowest unoccupied molecular orbitals (HOMO and LUMO, respectively) are modified upon adsorption, and new electronic states can be seen at the Fermi level. The DOS projected on the five C and the five Al atoms involved in the bonding shows that these additional states arise from strong sp hybridization (Figure 5c). At WF sites, the HOMO is shifted toward higher binding energies and the LUMO-derived band is shifted below the Fermi level, consistent with electron transfer from the substrate to C_{60} (Figure 5d). Interestingly, the shifts are larger than those usually observed for C_{60} on noble metal surfaces and differ at DS and WF sites. For an isolated C_{60}, it is known that the electron charge density is higher on 6:6 C−C bonds connecting hexagonal facets than on 6:5 C−C bonds connecting pentagonal and hexagonal facets.[28] The C atoms involved in the bonding appear to be those involved in 6:6 bonds at DS sites and in 6:5 bonds at WF sites. This suggests that the bonding is more favorable between electron-poor Al substrate

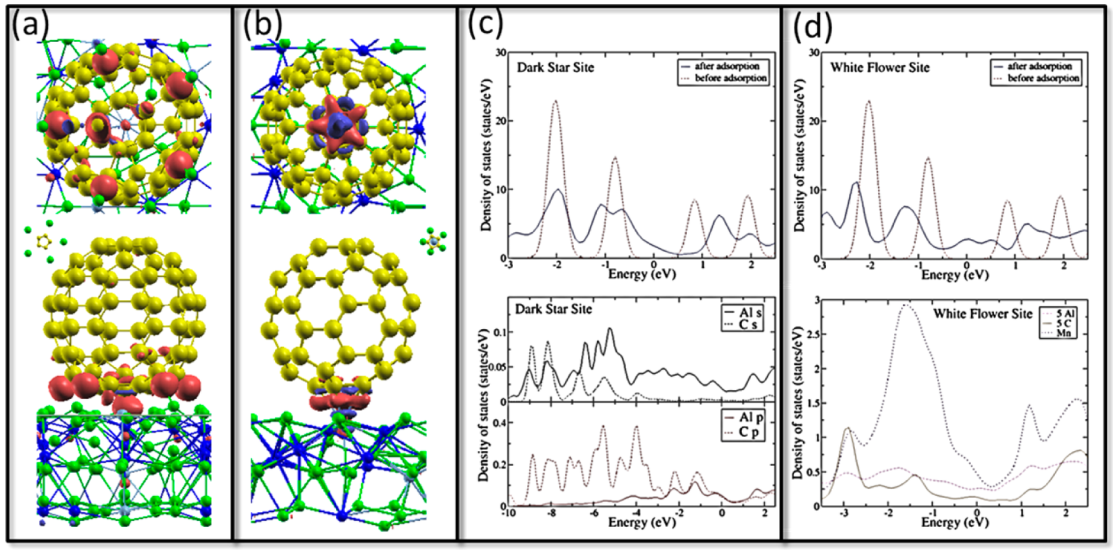

Figure 5. Isosurfaces of electron density difference for C_{60} adsorbed at DS site (a) and at WF site (b). Red areas represent electron accumulation zone, and blue areas are electron depletion zone. Al atoms are shown in green, Pd in dark blue, Mn in light blue, and C in yellow. The bottom images are side views, and top images are viewed from below the C_{60}. The isosurface value is $\pm 4 \times 10^{-3}$ e/nm^3. The relative positions of the bottom pentagonal C face with respect to the surface are shown in the central part. (c) Projected DOS on C_{60} at DS site before and after adsorption (top) and on one Al and C atom pair involved in the bonding (bottom) showing sp hybridization. (d) Projected DOS on C_{60} at WF site before and after adsorption (top) and on one of the five Al and C atom pairs and the Mn atom involved in the bonding (bottom).

atoms and electron-rich 6:6 bonds at DS sites as well as between the electron-rich Mn atom and the electron-deficient 6:5 bonds at WF sites. In agreement with this picture, the DOS projected on the five C atoms, the five Al atoms, and the Mn atom involved in the bonding at WF sites show strong spd hybridization between C and Mn atoms and a lesser degree of hybridization with the Al atoms.

CONCLUSION

In summary, we show that the complex potential energy landscape of quasicrystalline surfaces allows the templated self-assembly of C_{60} molecules into long-range quasiperiodic thin films. This is observed on four different Al-based quasicrystalline surfaces and thus appears to be rather general. The quasiperiodicity in the molecular films is mediated by preferred adsorption at specific quasilattice sites identified as truncated cluster sites exhibiting local 5-fold symmetry. Therefore symmetry matching at the molecule–substrate interface is an essential parameter in the determination of the preferred adsorption sites and the propagation of the quasiperiodic order into the molecular films. In addition, these sites are separated by distances that are compatible with intermolecular distances, avoiding strong van der Waals repulsion. At a local scale, DFT calculations indicate that the most favorable adsorption configurations at these sites correspond to molecules contacting the substrate with the electron-deficient pentagonal C face, allowing efficient electron transfer from the substrate to the C_{60}. This feature is probably specific to QC surfaces (and possibly to their approximants). Indeed C_{60} adsorption on normal crystalline surfaces allows symmetry matching only with either 2-fold or 3-fold symmetry axis, corresponding to adsorption geometries where the molecule lies either on a 6:6 C–C bond or on a hexagonal face.[28] On QC substrates, one expects most of the C_{60} to be adsorbed on a pentagonal C face, and this should influence the properties of the molecular film in a unique way. These results could be expanded by functionalizing the molecules to investigate the physical properties of model 2D quasiperiodic systems, for example to study magnetic frustration on a quasiperiodic lattice by using endohedral fullerenes with magnetic moments.

METHODS

The single crystals were grown either by the Bridgman method (*i*-$Al_{70}Pd_{21}Mn_9$), by a cyclic heat-treatment process (*i*-$Al_{65}Cu_{23}Fe_{12}$), or by the flux method (*d*-$Al_{63.2}Co_{19.5}Cu_{17.3}$ and *d*-$Al_{72.1}Ni_{10.6}Co_{17.3}$). Surfaces were oriented by back-Laue scattering. All experiments were performed in a commercial UHV system (MULTIPROBE; Omicron Nanotechnology, Taunusstein) equipped with LEED, variable-temperature STM, and photoemission spectroscopy. Clean surfaces were prepared by repeated cycles of sputtering (Ar^+, 2 keV) and annealing (*T* from 900 to 1020 K). The molecular films were grown by deposition at substrate temperature ranging from 623 to 673 K using a homemade evaporation source. The LEED patterns and STM images were recorded at room temperature. DFT calculations were performed using the Vienna *ab initio* simulation package (VASP).[26] The Kohn–Sham equations are solved in a plane-wave basis set, using the projector-augmented-wave (PAW) method to describe interactions between core and valence electrons. We used dispersion-corrected Kohn–Sham DFT energy functionals, where the conventional Kohn–Sham DFT energy functional is corrected by the DFT-D2 method.[27]

Conflict of Interest: The authors declare no competing financial interest.

Acknowledgment. M.C.d.W., D.M.W., and T.A.L. prepared the single crystals. V.F. and J.L. performed the experiments, while E.G. made the DFT calculations. V.F. wrote the paper, and all authors commented on the manuscript. We thank M. Krajčí for providing the structural model of the 2/1 rational approximant to the Al–Pd–Mn icosahedral QC. V.F., E.G., J.L., and M.C.d.W. acknowledge support by the ANR CAPRICE 2011-INTB-1001-01 and the European C-MAC consortium. T.A.L. and D.M.W. acknowledge support by the U.S. Department of Energy, Office of Basic Energy Science, Division of Materials Sciences and Engineering, under Contract No. DE-AC02-07CH11358.

REFERENCES AND NOTES

1. Shechtman, D.; Blech, I.; Gratias, D.; Cahn, J. Metallic Phase with Long-Range Orientational Order and No Translational Symmetry. *Phys. Rev. Lett.* **1984**, *53*, 1951–1953.
2. Janot, C. *Quasicrystals: A Primer*; Oxford University Press, 2012.
3. Zeng, X.; Ungar, G.; Liu, Y.; Percec, V.; Dulcey, A. E.; Hobbs, J. K. Supramolecular Dendritic Liquid Quasicrystals. *Nature* **2004**, *428*, 157–160.
4. Talapin, D. V.; Shevchenko, E. V.; Bordnarchuk, M. I.; Ye, X.; Chen, J.; Murray, C. B. Quasicrystalline Order In Self-Assembled Binary Nanoparticle Superlattices. *Nature* **2009**, *461*, 964–967.
5. Förster, S.; Meinel, K.; Hammer, R.; Trautmann, M.; Widdra, W. Quasicrystalline Structure Formation in a Classical Crystalline Thin-Film System. *Nature* **2013**, *502*, 216–218.
6. Johnston, J. C.; Kastelowitz, N.; Molinero, V. Liquid to Quasicrystal Transition in Bilayer Water. *J. Chem. Phys.* **2010**, *133*, 154516.
7. Gierer, M.; Van Hove, M. A.; Goldman, A. I.; Shen, Z.; Chang, S.-L.; Pinhero, P. J.; Jenks, C. J.; Anderegg, J. W.; Zhanh, C.-M.; Thiel, P. A. Fivefold Surface of Quasicrystalline AlPdMn: Structure Determination Using Low-Energy-Electron Diffraction. *Phys. Rev. B* **1998**, *57*, 7628–7641.
8. Thiel, P. A. Quasicrystal Surfaces. *Annu. Rev. Phys. Chem.* **2008**, *59*, 129–152.
9. Papodopoulos, Z.; Kasner, G.; Ledieu, J.; Cox, E. J.; Richardson, N. V.; Chen, Q.; Diehl, R. D.; Lograsso, T. A.; Ross, A. R.; McGrath, R. Bulk Termination of the Quasicrystalline Fivefold Surface of $Al_{70}Pd_{21}Mn_9$. *Phys. Rev. B* **2002**, *66*, 184207.
10. Unal, B.; Jenks, C. J.; Thiel, P. A. Adsorption Sites on Icosahedral Quasicrystal Surfaces: Dark Stars and White Flowers. *J. Phys.: Condens. Matter* **2009**, *21*, 055009.
11. Unal, B.; Jenks, C. J.; Thiel, P. A. Comparison between Experimental Surface Data and Bulk Structure Models for Quasicrystalline AlPdMn: Average Atomic Densities and Chemical Compositions. *Phys. Rev. B* **2008**, *77*, 195419.
12. Sharma, H. R.; Fournée, V.; Shimoda, M.; Ross, A. R.; Lograsso, T. A.; Tsai, A. P.; Yamamoto, A. Structure of The Fivefold Surface of the Icosahedral Al-Cu-Fe Quasicrystal: Experimental Evidence of Bulk Truncations at Larger Interlayer Spacings. *Phys. Rev. Lett.* **2004**, *93*, 165502.
13. Unal, B.; Fournée, V.; Schnitzenbaumer, K. J.; Ghosh, C.; Jenks, C. J.; Ross, A. R.; Lograsso, T. A.; Evans, J. W.; Thiel, P. A.

Nucleation and Growth of Ag Islands on Fivefold Al-Pd-Mn Quasicrystal Surfaces: Dependence of Island Density on Temperature and Flux. *Phys. Rev. B* **2007**, *75*, 064205.
14. Cai, T.; Ledieu, J.; McGrath, R.; Fournée, V.; Lograsso, T. A.; Ross, A. R.; Thiel, P. A. Pseudomorphic Starfish: Nucleation of Extrinsic Metal Atoms on a Quasicrystalline Substrate. *Surf. Sci.* **2003**, *526*, 115–120.
15. Ledieu, J.; Unsworth, P.; Lograsso, T. A.; Ross, A. R.; McGrath, R. Ordering of Si Atoms on the Fivefold Al-Pd-Mn Quasicrystal Surface. *Phys. Rev. B* **2006**, *73*, 012204.
16. Ledieu, J.; Leung, L.; Wearing, L. H.; McGrath, R.; Lograsso, T. A.; Wu, D.; Fournée, V. Self-assembly, Structure, and Electronic Properties of a Quasiperiodic Lead Monolayer. *Phys. Rev. B* **2008**, *77*, 073409.
17. Krajčí, M.; Hafner, J.; Ledieu, J.; Fournée, V.; McGrath, R. Quasiperiodic Pb Monolayer on the Fivefold i-Al-Pd-Mn Surface: Structure and Electronic Properties. *Phys. Rev. B* **2010**, *82*, 085417.
18. Sharma, H. R.; Nozawa, K.; Smerdon, J. A.; Nugent, P. J.; McLeod, I.; Dhanak, V. R.; Shimoda, M.; Ishii, Y.; Tsai, A. P.; McGrath, R. Templated Three-Dimensional Growth of Quasicrystalline Lead. *Nat. Commun.* **201**, *4*, 2715.
19. Ledieu, J.; Muryn, C. A.; Thornton, G.; Diehl, R. D.; Lograsso, T. A.; Delaney, D. W.; McGrath, R. C_{60} Adsorption on the Quasicrystalline Surface of $Al_{70}Pd_{21}Mn_9$. *Surf. Sci.* **2001**, *472*, 89–96.
20. Young, K. M.; Smerdon, J. A.; Sharma, H. R.; Lahti, M.; Pussi, K.; McGrath, R. Acene Adsorption on a Fibonacci-modulated Cu Film. *Phys. Rev. B* **2013**, *87*, 085407.
21. Deloudi, S.; Fleischer, F.; Steurer, W. Unifying Cluster-Based Structure Models of Decagonal Al-Co-Ni, Al-Co-Cu and Al-Fe-Ni. *Acta Crystallogr. B* **2011**, *67*, 1–17.
22. Kortan, A. R.; Becker, R. S.; Thiel, F. A.; Chen, H. S. Real Space Atomic Structure of a Two-Dimensional Decagonal Quasicrystal. *Phys. Rev. Lett.* **1990**, *64*, 200–203.
23. Zenkyu, R.; Yuhara, J.; Matsui, T.; Shah Zaman, S.; Schmid, M.; Varga, P. Composition and Local Atomic Arrangement of Decagonal Al-Co-Cu Quasicrystal Surfaces. *Phys. Rev. B* **2012**, *86*, 115422.
24. Quiquandon, M.; Gratias, D. Unique Six-Dimensional Structural Model for Al-Pd-Mn and Al-Cu-Fe Icosahedral Phases. *Phys. Rev. B* **2006**, *74*, 214205.
25. Krajčí, M.; Hafner, J. Structure, Stability, and Electronic Properties of the i-AlPdMn Quasicrystalline Surface. *Phys. Rev. B* **2005**, *71*, 054202.
26. Kresse, G.; Furthmüller, J. Efficient Iterative Schemes for ab Initio Total-Energy Calculations using a Plane-Wave Basis Set. *Phys. Rev. B* **2012**, *86*, 115422.
27. Grimme, S. Semiempirical GGA-Type Density Functional Constructed with a Long-Range Dispersion Correction. *J. Comput. Chem.* **2006**, *27*, 1787–1799.
28. Shi, X.-Q.; Van Hove, M. A.; Zhang, R.-Q Survey of Structural and Electronic Properties of C_{60} on Closed-Packed Metal Surfaces. *J. Matter Sci.* **2012**, *47*, 7341–7355.